Am J Physiol Heart Circ Physiol. Author manuscript; available in PMC 2016 December 08.

Published in final edited form as:

Am J Physiol Heart Circ Physiol. 2010 December ; 299(6): H1854–H1864. doi:10.1152/ajpheart.00595.2010.

Rescue treatment with a Rho-kinase inhibitor normalizes right ventricular function and reverses remodeling in juvenile rats with chronic pulmonary hypertension

Emily Z. Xu[1,5], **Crystal Kantores**[1], **Julijana Ivanovska**[1], **Doreen Engelberts**[2], **Brian P. Kavanagh**[2,4,5], **Patrick J. McNamara**[2,3], and **Robert P. Jankov**[1,3,5]

[1]Clinical Integrative Biology, Sunnybrook Research Institute, University of Toronto, Toronto, Ontario, Canada

[2]Physiology and Experimental Medicine Program, Hospital for Sick Children Research Institute, University of Toronto, Toronto, Ontario, Canada

[3]Division of Neonatology, Department of Paediatrics, University of Toronto, Toronto, Ontario, Canada

[4]Department of Anaesthesia, University of Toronto, Toronto, Ontario, Canada

[5]Department of Physiology, University of Toronto, Toronto, Ontario, Canada

Abstract

Chronic pulmonary hypertension in infancy and childhood is characterized by a fixed and progressive increase in pulmonary arterial pressure and resistance, pulmonary arterial remodeling, and right ventricular hypertrophy and systolic dysfunction. These abnormalities are replicated in neonatal rats chronically exposed to hypoxia from birth in which increased activity of Rho-kinase (ROCK) is critical to injury, as evidenced by preventive effects of ROCK inhibitors. Our objective in the present study was to examine the reversing effects of a late or rescue approach to treatment with a ROCK inhibitor on the pulmonary and cardiac manifestations of established chronic hypoxic pulmonary hypertension. Rat pups were exposed to air or hypoxia (13% O_2) from *postnatal day 1* and were treated with Y-27632 (15 mg/kg) or saline vehicle by twice daily subcutaneous injection commencing on *day 14*, for up to 7 days. Treatment with Y-27632 significantly attenuated right ventricular hypertrophy, reversed arterial wall remodeling, and completely normalized right ventricular systolic function in hypoxia-exposed animals. Reversal of arterial wall remodeling was accompanied by increased apoptosis and attenuated content of endothelin (ET)-1 and ET_A receptors. Treatment of primary cultured juvenile rat pulmonary artery smooth muscle cells with Y-27632 attenuated serum-stimulated ROCK activity and proliferation and increased apoptosis. Smooth muscle apoptosis was also induced by short interfering RNA-mediated knockdown of ROCK-II, but not of ROCK-I. We conclude that sustained rescue treatment with a ROCK inhibitor reversed both the hemodynamic and structural abnormalities of

Address for reprint requests and other correspondence: R. P. Jankov, Dept. of Newborn and Developmental Paediatrics, Sunnybrook Health Sciences Centre, 76 Grenville St., Toronto, Ontario M5S 1B2 Canada (robert.jankov@sunnybrook.ca).

DISCLOSURES

No conflicts of interest, financial or otherwise, are declared by the author(s).

chronic hypoxic pulmonary hypertension in juvenile rats and normalized right ventricular systolic function. Attenuated expression and activity of ET-1 and its A-type receptor on pulmonary arterial smooth muscle was a likely contributor to the stimulatory effects of ROCK inhibition on apoptosis. In addition, our data suggest that ROCK-II may be dominant in enhancing survival of pulmonary arterial smooth muscle.

Keywords

hypoxia; endothelin-1; apoptosis; smooth muscle cells

Chronic pulmonary hypertension (PHT) is a rare but debilitating and fatal disease in infants and children, most frequently observed in the settings of severe bronchopulmonary dysplasia (46, 60), congenital diaphragmatic hernia (39), structural heart diseases with increased pulmonary blood flow (18, 48), and persistent PHT of the newborn (41). Current efforts to treat chronic PHT in this population are hampered by frequent nonresponsiveness to currently available pulmonary vasodilators and a rapid (when compared with adults) progression toward end-stage pathology, characterized by severe vascular remodeling and right ventricular (RV) dysfunction (8, 17, 63). Despite an expanding range of therapeutic options (3, 63), newer treatments may not lead to sustained improvements in symptoms or to an overall increase in longevity (63); therefore, the prognosis for this condition remains poor.

Activation of the small GTPase, RhoA, and its effector protein, Rho-kinase (ROCK) (36, 57), are strongly implicated as a key pathway regulating pulmonary vascular tone and smooth muscle phenotype. ROCK activation leads to Ca^{++} sensitization and thereby contraction of smooth muscle through phosphorylation of myosin regulatory light chain (MLC) (12, 56). This appreciation has led to the experimental use of ROCK-specific kinase inhibitors, among which include Y-27632 (21) and fasudil (53), as therapeutic vasodilators. In adult models, these agents have been reported to inhibit sustained pulmonary vasoconstriction in response to acute and chronic hypoxia (11, 50), vaso-occlusive PHT (45), and infusion of a variety of vasoconstrictors acting upon G protein-coupled receptors, including endothelin (ET)-1 (5, 54, 64). Furthermore, pilot data in humans have confirmed that ROCK inhibitors are equal or superior to existing pulmonary vasodilators in both adults (20, 42) and children (33).

Our group has previously shown that the RhoA/ROCK pathway is activated in pulmonary arteries of neonatal rats with hypoxia- or bleomycin-induced PHT (38). In both models, a single bolus of ROCK inhibitor (Y-27632 or fasudil) completely normalized pulmonary vascular resistance (PVR) (38). We subsequently reported that sustained ROCK inhibition from birth prevented chronic hypoxia-induced vascular remodeling, through inhibitory effects on arterial wall smooth muscle proliferation (68), suggesting that ROCK may regulate, at the transcriptional level, the expression of key mediators leading to pulmonary vascular remodeling (37, 44).

The aim of the present study was to determine whether prolonged rescue treatment with a ROCK inhibitor (i.e., sustained treatment commenced after chronic PHT is already

established) would lead to sustained pulmonary vasodilatation, reversal of vascular remodeling, and restoration of RV function in chronic hypoxia-exposed juvenile rats. In the newborn rat, ET-1 functions not only as a potent vasoconstrictor but also as a survival factor for pulmonary artery smooth muscle cells (PASMCs), through its effects on the ET_A receptor (22). We therefore hypothesized that any reversing effects of ROCK inhibition on pulmonary arterial (PA) wall remodeling, presumably through enhanced smooth muscle apoptosis, would be accompanied by attenuated ET-1 and/or ET_A receptor expression. Finally, given the importance of right heart function to survival in chronic PHT (6), we examined the effects of sustained ROCK inhibition on diminished RV systolic performance, which we previously determined to be unaffected by a single bolus dose of ROCK inhibitor (38).

MATERIALS AND METHODS

Materials

Y-27632 and fasudil (HA-1077) were from Alexis Biochemicals (San Diego, CA) and LC Laboratories (Woburn, MA), respectively. Phos-tag acrylamide was from Nard Institute (Amagasaki City, Hyogo, Japan). Cell Death Detection ELISA and dUTP TUNEL assay kits were from Roche (Laval, Québec, Canada). Bromodeoxyuridine (BrdU) cell proliferation colorimetric assay kits were from Exalpha Biologicals (Shirley, MA). WST-8 colorimetric assay kits were from Cayman Chemical (Ann Arbor, MI). DMEM, trypsin, and heat-inactivated FBS were from Gibco (Burlington, Ontario, Canada). Avidin-biotin-peroxidase complex immunohistochemistry kits, 6-diamino-2′-phenylindole aqueous mounting medium, and 3,3′ diaminobenzidine staining kits were from Vector Laboratories (Burlingame, CA). Weigert's resorcin-fuchsin stain was from Rowley Biochemical (Danvers, MA). GAPDH (Catalog No. sc-25778), MLC (Catalog No. sc-15370), ROCK-I (Catalog No. sc-17794), cleaved ROCK-I (Catalog No. sc-52953), and goat anti-rabbit and -mouse IgG-biotin antibodies were from Santa Cruz Biotechnology (Santa Cruz, CA). Anti-ROCK-II (Catalog No. 610624) was from BD Biosciences (Mississauga, Ontario, Canada). Anti-α-smooth muscle actin (Catalog No. MS-113-PI) and prepro-ET-1 (Catalog No. MA3-005) were from Thermo Fisher Scientific (Ottawa, Ontario, Canada). Anti-ET_A receptor (Catalog No. NBP1-00818) was from Novus Biologicals (Littleton, CO). Antiphosphorylated Thr850 myosin phosphatase target (MYPT)-1 (Catalog No. 36-003) and pan-MYPT-1 (Catalog No. 07-672) were from Upstate/Millipore (Billerica, MA). Anti-cleaved caspase-3 (Catalog No. 9661) and goat anti-rabbit and anti-mouse immunoglobulin (IgG)-peroxidase antibodies were from Cell Signaling Technology (Beverly, MA). Predesigned rat short-interfering RNAs (siRNAs) were purchased from Ambion/Applied Biosystems (Austin, TX). Custom primers for quantitative RT-PCR (qRT-PCR) were from Integrated DNA Technologies (Skokie, IL). Unless otherwise specified, all other chemicals and reagents were from Sigma Aldrich (Oakville, Ontario, Canada).

Animal exposures and interventions

All procedures involving animals were performed in accordance with the standards of the Canadian Council on Animal Care and were approved by the Animal Care Committee of the Sunnybrook Research Institute. Timed-pregnant Sprague-Dawley rats (150–200 g) were

purchased from Taconic Farms (Germantown, NY). Each litter was nursed in either air (21% O_2) or hypoxia (13% O_2), from *postnatal day 1*, for up to 21 days, as previously described in detail (28). From *day 14*, pups received Y-27632 [15 mg/kg; 3 mg/ml suspended in 0.9% (wt/vol) saline vehicle = 5 μl/g body wt] or an equivalent volume of vehicle alone by twice daily subcutaneous injection for either 2 (to *day 16* of life) or 7 (to *day 21* of life) days. Doses of 15 mg/kg Y-27632 or 30 mg/kg (but not 15 mg/kg) fasudil were previously shown to normalize PVR in pups exposed to acute or chronic hypoxia (38). In preliminary dose response studies (15 or 30 mg/kg ip twice daily), we compared the effects of Y-27632 and fasudil, commencing on *day 14*. No mortality resulted from 15 mg/kg Y-27632; however, treatment with 15 mg/kg fasudil led to ~30% mortality, all during the first 2 days of treatment. Death was preceded by a rapid onset of gray pallor and decreased activity, within minutes of injection, which we interpreted as signs of hypotensive shock. Treatment with 30 mg/kg of either drug led to increased mortality, with fasudil causing a higher rate than Y-27632 (~90% vs. ~ 40%, also predominantly within the first 2 days of treatment; data not shown). These effects are consistent with a known lack of pulmonary selectivity of ROCK inhibitors, leading to parallel systemic hypotension (7). We elected to employ Y-27632 for the present studies due to an inability to completely inhibit ROCK activity in the lung without causing excess mortality with fasudil (data not shown); however, we acknowledge that fasudil remains the only ROCK inhibitor to have thus far been tested in humans (20, 33). A twice daily dosing regimen was undertaken based upon in vivo work by others suggesting that vasodilatory activity of Y-27632 in adult rats lasts 6–12 h following a single enteral dose (42).

Equal litter sizes (10–12 pups) and sex distribution were maintained throughout the exposure period. Food and water were available ad libitum. Dams were exchanged daily between paired air and hypoxia chambers to prevent any maternal toxicity and consequent nutritional effects on the pups. At the end of each exposure period, pups were euthanized either by exsanguination after anesthesia or by pentobarbital sodium overdose. Except for a subset of animals in which the longevity of effects on pulmonary hemodynamics was examined, all animals received the last dose of Y-27632 within 1 h of euthanization.

Cardiac ventricular weights

RV hypertrophy (RVH) was quantified by measuring the RV to left ventricle and septum (LV + S) weight ratio (Fulton index), as previously described (25).

Two-dimensional echocardiography-derived measurements of pulmonary hemodynamics

Pulmonary hemodynamics were evaluated noninvasively using two-dimensional echocardiography and Doppler ultrasound (Vivid 7 cardiac ultrasound system and I13L linear probe; GE Medical Systems, Milwaukee, WI), as previously described in detail (38). Animals were anesthetized with ketamine-xylazine and spontaneously breathing room air at the time of the study. For estimation of PVR, a short-axis view at the level of the aortic valve was obtained and the pulmonary artery identified by color flow Doppler. The PA acceleration time (PAAT) was measured as the time from the onset of systolic flow to peak pulmonary outflow velocity, and the RV ejection time (RVET) was measured as the time from onset to completion of systolic pulmonary flow. PVR was estimated using the formula:

[1/(PAAT/RVET)] (38). Pulmonary artery systolic pressure (PASP) was calculated using the formula: PASP = 137.2 − (3.3 × PAAT) (27). For estimation of RV stroke volume, the PA diameter was measured by color flow Doppler at the hinge-point of the pulmonary valve leaflets. From the same Doppler interrogation of the pulmonary artery used to measure PAAT and RVET, RV output was calculated using the formula: $(\text{PA diameter}/2)^2 \times 3.14 \times$ PA velocity time integral × heart rate (beats/min). PA velocity time integral was measured by tracing the leading edge of the velocity time graph from the onset to completion of systolic pulmonary flow. RV output (in ml/min) was corrected for body weight to derive a RV performance index (in $\text{ml}\cdot\text{min}^{-1}\cdot\text{kg}^{-1}$). LV systolic performance was estimated from the parasternal short-axis view by calculating the shortening fraction according to the formula: [(LV end-diastolic diameter − LV systolic diameter)]/LV end-diastolic diameter × 100.

Measurement of RV systolic pressure

Rat pups were anesthetized with ketamine-xylazine, tracheotomized, and placed on a volume-controlled intermittent positive-pressure ventilator (Model 687; Harvard Apparatus, Holliston, MA) set at 90 breaths/min, 10 ml/kg tidal volume, and FiO_2 0.21. The thorax was opened and the ventral portion of the ribcage was removed, after which a 23-gauge saline-filled needle attached to a pressure transducer was inserted into the RV lumen. Pressure was captured by computer using Labchart software (version 5.1; AD Instruments, Colorado Springs, CO), and the highest stable RV systolic pressure (RVSP) was recorded for each animal.

Measurement of systemic blood pressure

Systemic blood pressure was noninvasively measured in anesthetized *day 21* rat pups using a tail cuff Doppler device (LE5002; Harvard Apparatus) at baseline and 15 min after treatment with intraperitoneal Y-27632, 15 mg/kg fasudil, or an equivalent volume of saline vehicle. Because of technical limitations of the device in smaller animals, reliable recordings were only possible in pups weighing >50 g, which precluded successful measurements in animals chronically exposed to hypoxia for 21 days, due to resultant growth restriction.

Histological studies

Lungs from four animals from each group (2 from each of 2 separate litters) were air-inflated and perfusion-fixed at constant pressure, embedded in paraffin, sectioned, and immunostained for α-smooth muscle actin, as previously described in detail (25). For assessment of percent arterial medial wall thickness (MWT), pulmonary arterioles (ranging from 20 to 100 μm external diameter), identified by the presence of both inner and outer elastic lamina using Weigert's resorcin-fuchsin stain (Rowley Biochemical, Danvers, MA), were digitally captured (Pixera Penguin 600CL; San Jose, CA) and measured by an observer blinded to group identity, as previously described in detail (28). Mean external diameter (taken as the outer elastic lamina) was calculated from measurements of round and ovoid vessels in two perpendicular planes to account for any irregularities in vessel shape, while excluding vessels that were cut tangentially (>3-fold difference in MWT between perpendicular planes). Percent MWT was calculated using the formula: ([2 × MWT]/mean external diameter) × 100.

qRT-PCR

RNA was extracted (Absolutely RNA Miniprep Kit; Agilent/Stratagene, La Jolla, CA) and reverse transcribed (Affinity-Script; Agilent) from lung tissue samples stored in RNALater (Applied Biosystems, Streetsville, Ontario, Canada). qRT-PCR was performed on a Stratagene MX3000P qPCR system using SYBR Green qPCR Master Mix (SA Biosciences, Frederick, MD). Cycling conditions were 95°C for 10 min followed by 40 cycles of 95°C for 15 s and 60°C for 60 s. A standard curve for each primer set was run, using a rat lung cDNA standard (Agilent), to ensure that reaction efficiency was equivalent to primers for the housekeeping gene, β-actin, the expression of which was determined in preliminary experiments to be unaffected by the experimental conditions. Following each standard curve reaction, molecular weight standards (O'GeneRuler; Fermentas, Burlington, Ontario, Canada) and PCR products underwent DNA gel electrophoresis to confirm the presence of a single product of predicted length. Primer sequences are listed in Table 1. A dissociation (melt) curve and a no-template control were run for each set of samples to exclude nonspecific product formation and reaction contamination. Samples were run in duplicate, and expression of the gene of interest was normalized to β-actin. Fold or fraction change in expression relative to calibrator (air-exposed vehicle-treated) samples was calculated by the $2^{-\Delta\Delta ct}$ method using Stratagene MxPro software (version 4.01).

Assessment of proliferation, apoptosis, and viability of PASMCs

Primary PASMC-enriched cultures (identified by their characteristic hill-and-valley morphology and positive immunostaining for calponin) were obtained from explants of pooled intrapulmonary arteries from *day 14* Sprague-Dawley rat pups, as previously reported in detail (22). Cells were passaged by trypsinization using 0.05% (wt/vol) trypsin/EDTA and centrifugation at 300 *g* for 5 min, followed by reseeding in 96-well plates. For examination of effects of Y-27632, equal numbers (1×10^5) of *passages 3–5* cells, suspended in DMEM + 10% (vol/vol) FBS, were seeded per well, allowed to attach, and grown to subconfluence (~70%), after which they were serum starved for 24 h in DMEM + 0.1% (vol/vol) FBS. Before assays of ROCK activity, proliferation, apoptosis, and cell survival, 6 wells/group were treated with DMEM + 0.1% (vol/vol) FBS (negative control group), DMEM + 10% (vol/vol) FBS (positive control group for assessment of ROCK activity, cell proliferation, and viability), DMEM + 10% (vol/vol) FBS and various concentrations of Y-27632 (0.1, 1, or 10 μM), or DMEM + 10% (vol/vol) FBS and paclitaxel (10 μM; positive control group for apoptosis assay). Treatments were for 24 h at a gas phase of 74% N_2-21% O_2-5% CO_2. All assays were performed in duplicate on cells derived from a different litter to ensure reproducibility of results. Proliferation (BrdU incorporation; Exalpha Biologicals), apoptosis (single-stranded DNA; Roche), and viability (WST-8; Cayman) were assayed using commercially available colorimetric kits, according to the manufacturer's instructions. The latter assay utilizes color change of a nontoxic tetrazolium-like compound as a reflection of live cell number.

siRNA-mediated gene knockdown

Passages 3–5 PASMCs were suspended (1.5×10^5/ml) in electroporation buffer (Ambion) containing 50 nM negative control (Catalog No. AM4611), ROCK I (Catalog No. 4390771;

ID No. s135694), or ROCK II (Catalog No. 4390771; ID No. s130059) Silencer Select siRNAs, and electroporated (BTX ECM 830; Harvard Apparatus) using a single 100 μS pulse at 1.5 kV/cm, after which they were added to a 10-fold excess of DMEM + 15% (vol/vol) FBS [medium changed for DMEM + 25% (vol/vol) FBS after 24 h] and allowed to attach. Efficacy in knockdown and absence of significant cytotoxicity under these electroporation conditions was established in preliminary experiments using prevalidated rat GAPDH positive control siRNA (Ambion, Catalog No. AM4624). After 48 h, cells were collected for RNA purification, reverse transcription, and qRT-PCR to confirm gene knockdown, as described above, or apoptosis was quantified using a plate-based assay (Roche).

Western blot analyses

Third or fourth generation intrapulmonary arteries were dissected from four litters per group (the pooled vessels of 2 animals from each litter representing 1 sample). PA tissue or PASMCs were lysed in RIPA buffer with protease [Protease Inhibitor Cocktail Set I (Catalog No. 539131); Calbiochem, San Diego, CA] and phosphatase [Phosphatase Inhibitor Cocktail Set 2 (Catalog No. P5726); Sigma] inhibitors and sonicated on ice at 40W for 30 s. Protein samples (50 μg/lane) were boiled in Laemmli buffer, fractionated by SDS-PAGE on 4–20% gradient Tris-glycine gels, transferred to polyvinylidene difluoride membranes, and blotted, as previously described (23). Dilutions of primary antisera were 1:750 for anti-ET_A receptor (50 kDa), 1:1,000 for cleaved caspase-3 (17 kDa), phospho- and pan-MYPT-1 (80 kDa) and cleaved ROCK-I (130 kDa), 1:2,000 for ROCK-I (150 kDa) and ROCK-II (160 kDa), 1:3,000 for prepro-ET-1 (24 kDa), and 1:5,000 for GAPDH (37 kDa). Phospho- and pan-MYPT-1, cleaved ROCK-I, and ROCK-I and -II content were examined in PA tissue collected on *day 21*. Prepro-ET-1, ET_A receptor, and cleaved caspase-3 protein contents were examined in pulmonary arteries collected on *day 16*. The earlier time point was arbitrarily chosen based on preliminary data indicating that changes in markers of apoptosis were not evident on *day 21*. Protein bands were identified using enhanced chemiluminescent substrate (Immobilon; Millipore) and exposure of blots to Blue Film (CL-XPosure; Pierce/Thermo Fisher Scientific). Bands were quantified by digital densitometry of nonsaturated radiographs with the background density removed (ImageJ; National Institutes of Health, Bethesda, MD). Differences in protein loading were compensated for by reblotting for GAPDH, the expression of which we have previously shown to be unaffected by chronic exposure to hypoxia (24, 28). MLC phosphorylation, as a marker of ROCK activity, was quantified by Phos-tag acrylamide SDS-PAGE (31) at *day 21*, as previously described (68). Following electrophoresis and transfer, membranes were blotted with anti-MLC at a dilution of 1:1,000, yielding two bands with Phos-tag (an upper band representing phosphorylated and a lower band representing unphosphorylated MLC) and only one band (20 kDa) when Phos-tag was omitted from the resolving gel (68). Density of the upper band was expressed as a ratio of the combined densities of both upper and lower bands.

In situ examination of apoptosis

Day 16 lung tissue was snap frozen in optimum cutting temperature (OCT) compound, as previously described (22), and then cut by cryostat into 12-μm sections, which were mounted and stored at −80°C until analysis. Apoptotic nuclei were labeled using a

commercially available fluorescein TUNEL enzymatic assay kit (Roche) and imaged using an epifluorescent microscope (Zeiss Axioskop, Oberkochen, Germany) with appropriate filter sets.

Data presentation and analysis

All values are expressed as means ± SE. Statistical significance ($P < 0.05$) was determined by one-way ANOVA followed by pairwise multiple comparisons using the Tukey test, where three or more groups were compared, and by unpaired *t*-test or Mann-Whitney rank sum test, where two groups were compared (SigmaPlot 11.0; Systat software, San Jose, CA).

RESULTS

Body and lung weights

Exposure to hypoxia for 21 days significantly decreased body weight relative to air-exposed controls (43.7 ± 0.8 g vs. 51.4 ± 1.0 g; $P < 0.001$, $n = 12$ animals/group). Treatment with Y-27632 from *days 14* to *21* did not alter body weights in either air-exposed (49.7 ± 0.8 g) or hypoxia-exposed (40.9 ± 0.6 g) animals ($P > 0.05$ compared with respective controls, $n = 12$ animals/group). Exposure to hypoxia also led to significantly decreased lung weight relative to air-exposed controls (716 ± 16 mg vs. 822 ± 23 mg; $P < 0.001$, $n = 12$ animals/group). Treatment with Y-27632 did not change lung weights in either air-exposed (810 ± 32 mg) or hypoxia-exposed (732 ± 24 mg) animals ($P > 0.05$ compared with respective controls, $n = 12$ animals/group).

RVSP, pulmonary hemodynamics, systemic blood pressure, and left ventricular contractility

Exposure to hypoxia for 21 days led to persistently increased PVR (Fig. 1*A*), PASP (Fig. 1*B*), RVSP (Fig. 1*C*), and decreased RV performance index (Fig. 1*D*) when examined in room air. Treatment of hypoxia-exposed animals with Y-27632 from *days 14* to *21* (within 1 h of the last dose; <1 h) normalized PVR (Fig. 1*A*), significantly attenuated PASP (Fig. 1*B*) and RVSP (Fig. 1*C*), and restored RV performance index to normal levels (Fig. 1*D*). RV performance index values remained normalized when examined 12–18 h (>12 h) after the last dose of Y-27632 (Fig. 1*D*) in contrast with improvements in PVR (Fig. 1*A*), PASP (Fig. 1*B*), and RVSP (Fig. 1*C*), which were not sustained. Since heart rate did not differ between groups ($P = 0.9$, by ANOVA; data not shown), RV stroke volume was the main variable, which accounted for differences in RV performance index. When compared with baseline, mean systemic blood pressure was significantly ($P < 0.05$, by *t*-test) decreased by treatment with either Y-27632 (−32 ± 3%; $n = 5$) or fasudil (−31 ± 2%; $n = 4$), whereas an equivalent volume of saline vehicle had no effect (+2 ± 0.3%; $P = 0.9$, $n = 5$). Neither exposure to hypoxia nor treatment with Y-27632 led to any significant changes in LV systolic performance ($P = 0.2$, by ANOVA; data not shown).

Structural changes of PHT

Exposure to hypoxia for 21 days led to significant RVH (Fig. 2*A*), increased MWT (Fig. 2*B*), and decreased luminal area (Fig. 2*C*) in pulmonary resistance arteries, consistent with inward remodeling causing partial luminal obstruction. Treatment of hypoxia-exposed

animals with Y-27632 from *days 14* to *21* significantly attenuated RVH (Fig. 2*A*), and normalized percent MWT (Fig. 2*B*). Interestingly, percentage MWT in air-exposed animals was also significantly decreased by treatment with Y-27632 (Fig. 2*B*). Relative changes in PA smooth muscle mass and MWT between groups are further illustrated by medium-power images of α-smooth muscle actin immunostaining of lung tissue (Fig. 2*C*) and high-power images of Hart's elastin-stained small pulmonary arteries (Fig. 2*D*).

ROCK activity and content in pulmonary arteries

Exposure to hypoxia for 21 days increased ROCK activity, as quantified by increased MLC phosphorylation ratio (Fig. 3*A*) and phosphorylated MYPT-1 content (Fig. 3*B*). Both were completely normalized by treatment with Y-27632 (Fig. 3, *A* and *B*). Neither exposure to hypoxia nor treatment with Y-27632 caused any significant changes in ROCK-I (Fig. 3*C*), ROCK-II (Fig. 3*D*), or cleaved ROCK-I (data not shown) content.

Lung expression and PA content of prepro-ET-1 and ET receptors

As shown in Table 2, whole lung mRNA expression of prepro-ET-1 and ET_A or ET_B receptors were quantified following treatment with either vehicle or Y-27632 for 2 days (*day 16*). Exposure to hypoxia from *days 1* to *16* led to significantly increased ET-1 expression, with no significant changes in expression of either ET_A or ET_B receptors. Treatment of hypoxia-exposed animals with Y-27632 normalized ET-1 expression. Expression of ET_A (but not ET_B) receptor was significantly decreased in both air- and hypoxia-exposed animals by Y-27632 (Table 2). Western blot analyses of PA prepro-ET-1 (Fig. 4*A*) or ET_A receptor (Fig. 4*B*) demonstrated increased content in vehicle-treated hypoxia-exposed animals, relative to air controls. Treatment with Y-27632 normalized both prepro-ET-1 and ET_A receptor content in hypoxia-exposed animals. Furthermore, ET_A receptor content was significantly decreased in air-exposed Y-27632 animals, relative to vehicle-treated controls (Fig. 4*B*).

Effects of Y-27632 on markers of apoptosis in pulmonary arteries

Representative in situ TUNEL staining is shown in Fig. 5*A*, demonstrating the presence of TUNEL-positive nuclei on the vascular walls of both air- and hypoxia-exposed animals treated with Y-27632, not evident in animals treated with vehicle. As shown in Fig. 5*B*, treatment with Y-27632 greatly increased cleaved caspase-3 content in both air- and hypoxia-exposed groups, relative to vehicle-treated controls (Fig. 5*B*).

Effects of Y-27632 on proliferation, apoptosis, and viability in primary cultured PASMCs

ROCK activity was increased in serum-stimulated PASMCs and completely suppressed by treatment with 10 μM Y-27632, as indicated by changes in Thr850 phosphorylation of the ROCK target, MYPT-1 (Fig. 6*A*). Treatment of PASMCs with Y-27632 (0.1, 1.0, or 10 μM) completely attenuated serum-induced proliferation (Fig. 6*B*), whereas 10 μM Y-27632 significantly increased apoptosis (Fig. 6*C*). These changes were paralleled by reduced cell viability with increasing doses of Y-27632 (Fig. 6*D*).

Effects of siRNA-mediated knockdown of ROCK isoforms on apoptosis in primary cultured PASMCs

When compared with negative control (scrambled) siRNA, which had no significant effect on ROCK-I or -II isoform expression compared with cells electroporated without siRNA ($P > 0.05$; data not shown), effective knockdown was achieved with ROCK-I or -II-specific siRNAs (Fig. 7*A*). PASMC apoptosis was greatly increased by knockdown of ROCK-II, whereas knockdown of ROCK-I had no effect (Fig. 7*B*).

DISCUSSION

Our main findings were that sustained rescue treatment with Y-27632 reversed arterial wall remodeling, decreased RVH, and restored RV systolic function in chronic hypoxia-exposed juvenile rats. Reversing effects on vascular remodeling of another ROCK inhibitor, fasudil, have been previously reported in adult rats with monocrotaline-induced chronic PHT (1, 40). To our knowledge, this is the first study to examine the reversing effects of ROCK inhibition on vascular remodeling in the immature animal, which may be more resistant to reversal than adults (8, 17, 29, 30, 47, 52, 62) and the first to document normalized RV function as a consequence of sustained rescue treatment with a ROCK inhibitor. Our observation that sustained reduction of PVR and of RVSP were dependent upon ongoing inhibition of ROCK activity with Y-27632 are further in keeping with ROCK-mediated pulmonary vasoconstriction being the main determinant of raised pulmonary vascular pressure and resistance secondary to chronic hypoxia (38, 58).

Compensated right heart function is the main determinant of longevity in chronic PHT (6). Since ROCK is highly expressed in myocardium (35) and the RhoA/ROCK pathway is known to be an important mediator of the hypertrophic responses of cardiomyocytes (67), it was conceivable that ROCK inhibition could have adversely affected function of the normal or remodeled RV. Our observations were that ROCK inhibition decreased RVH and completely normalized RV output, while having no adverse effects on LV contractility or on RV function in normal (air-exposed) animals. These findings suggest that ROCK inhibitors have potential to improve survival in chronic PHT and add to previously identified beneficial effects of ROCK inhibition on LV dysfunction secondary to ischemia-reperfusion injury (16), chronic hypertension (32), and diabetes (34). Interestingly, beneficial effects of sustained treatment with Y-27632 on RV output remained present in the face of raised pulmonary vascular pressure and resistance, raising the possibility that this effect may have been contributed to by factors other than decreased pressure load or acute changes in ROCK activity within the heart. Downstream mediators of ROCK, which may account for such improvements in RV function, remain unknown and await exploration in future studies.

We observed that ROCK inhibition led to attenuated serum-induced proliferation in vitro and increased apoptosis of PA smooth muscle both in vitro and in vivo. Stimulatory effects on PA smooth muscle apoptosis secondary to Y-27632 were observed in both air- and hypoxia-exposed groups, leading to significant reductions in thickness of the medial arterial wall. Increased apoptosis appeared to be selective for pulmonary arteries, since total lung weight was not affected by treatment and TUNEL-positive nuclei in the proximal and distal airways were not obviously increased by Y-27632 (data not shown). These findings are consistent

with previous work demonstrating proapoptotic effects of ROCK inhibitors on vascular smooth muscle (2) and either no effect, or antiapoptotic effects, on other cell types (55). Currently available ROCK inhibitors are not isoform-specific (9); therefore, it was not possible to determine the relative contribution of each isoform to ROCK-mediated effects in vivo. However, using siRNA-mediated inhibition of gene function in vitro, we derived the new insight that ROCK-II may be the dominant isoform accounting for ROCK-mediated effects on PASMC survival.

Activation of the ET_A receptor is known to be critical to chronic hypoxia-induced vascular remodeling in the neonatal mouse (4) and rat (28) and appears to be an important mediator of chronic PHT in human infants (10, 51). We therefore examined changes in prepro-ET-1 and ET_A receptor content in pulmonary arteries and found that upregulated content in hypoxia-exposed animals was completely attenuated by treatment with Y-27632. ET_A receptor was also decreased in air-exposed animals by Y-27632. In previous work, we have reported that ET-1 is a potent survival factor (but not a mitogen) for neonatal rat PASMCs (22). We also observed that ET_A receptor blockade increased neonatal rat PASMC apoptosis (22). Therefore, we speculate that changes in expression pattern of the ET-1/ET_A receptor axis may have contributed toward increased apoptosis secondary to treatment with Y-27632, in both air- and hypoxia-exposed animals. In addition, earlier work has shown that ROCK mediates PASMC production of ET-1 (66), suggesting that a feed-forward autocrine/paracrine loop between ROCK and ET-1 may exist in juvenile rat PASMCs, potentially leading to amplified effects on their growth and survival. Attenuation of ET-1-induced antiapoptotic effects is likely to be one, but not the only, mechanism by which ROCK inhibition may reverse remodeling. Another possible pathway to be explored is augmented nitric oxide (NO)-cGMP signaling (2, 13, 26), which may also regulate smooth muscle growth and survival (61). Indeed, reciprocal interactions between the RhoA/ROCK, NO-cGMP, and ET-1 pathways are suggested by reported benefits of augmented NO-cGMP or attenuated ET-1 signaling on pulmonary vascular injury in experimental animals, which have been attributed, at least in part, to inhibitory effects on the RhoA/ROCK pathway (15, 19, 40, 43, 49).

An adverse consequence of systemically administered Y-27632, also reported in adult rats (7), was parallel dilation of the systemic vasculature, leading to systemic hypotension. Systemic effects have been limited, in adult rats, by direct delivery of ROCK inhibitor to the lung (42). Despite significant effects on systemic blood pressure, we observed no adverse effects on somatic growth, in contrast with previously reported effects of ROCK inhibitors when administered from birth (68). Interestingly, although Y-27632 is a more potent ROCK inhibitor than fasudil (9), effects on systemic blood pressure were equivalent, suggesting that inhibition of other kinases (59) or another off-target effect may have contributed to hypotension and increased mortality secondary to fasudil. Newer kinase inhibitors (e.g., H-1152) with greater specificity toward ROCK than either Y-27632 or fasudil are available and have been successfully employed in short-term in vivo studies (34), although their comparative effects on pulmonary and systemic vascular resistance and longer term effects have yet to be examined. Furthermore, although ROCK inhibitors are highly effective at normalizing pulmonary vascular pressure and resistance in multiple experimental models,

other experimental therapies [e.g., stimulators/activators of soluble guanylate cyclase (14, 65)] appear to be equally efficacious.

Chronic PHT in early life is caused by an heterogeneous group of disorders with multiple factors contributing to pathogenesis, including inflammation, increased pulmonary blood flow, and pulmonary vascular hypoplasia, which the present model does not replicate (38). Therefore, our observations require confirmation in neonatal models where such factors are contributory. In addition, further studies are required to determine whether reversal of vascular remodeling confers any benefit upon pulmonary hemodynamics in the longer term and whether beneficial effects on RV function last well beyond the treatment period.

Acknowledgments

GRANTS

R. P. Jankov is a Canadian Institutes of Health Research (CIHR) New Investigator. This work was supported by operating funding from the CIHR (MOP-84290) and infrastructure funding from the Canada Foundation for Innovation.

References

1. Abe K, Shimokawa H, Morikawa K, Uwatoku T, Oi K, Matsumoto Y, Hattori T, Nakashima Y, Kaibuchi K, Sueishi K, Takeshit A. Long-term treatment with a Rho-kinase inhibitor improves monocrotaline-induced fatal pulmonary hypertension in rats. Circ Res. 2004; 94:385–393. [PubMed: 14670839]
2. Abe K, Tawara S, Oi K, Hizume T, Uwatoku T, Fukumoto Y, Kaibuchi K, Shimokawa H. Long-term inhibition of Rho-kinase ameliorates hypoxia-induced pulmonary hypertension in mice. J Cardiovasc Pharmacol. 2006; 48:280–285. [PubMed: 17204906]
3. Abman SH. Pulmonary hypertension in older children: new approaches and therapies. Paediatr Respir Rev. 2006; 7(Suppl 1):S177–S179. [PubMed: 16798555]
4. Ambalavanan N, Bulger A, Murphy-Ullrich J, Oparil S, Chen YF. Endothelin-A receptor blockade prevents and partially reverses neonatal hypoxic pulmonary vascular remodeling. Pediatr Res. 2005; 57:631–636. [PubMed: 15774824]
5. Barman SA. Vasoconstrictor effect of endothelin-1 on hypertensive pulmonary arterial smooth muscle involves Rho-kinase and protein kinase C. Am J Physiol Lung Cell Mol Physiol. 2007; 293:L472–L479. [PubMed: 17468135]
6. Bogaard HJ, Abe K, Vonk Noordegraaf A, Voelkel NF. The right ventricle under pressure: cellular and molecular mechanisms of right-heart failure in pulmonary hypertension. Chest. 2009; 135:794–804. [PubMed: 19265089]
7. Casey DB, Badejo AM, Dhaliwal JS, Sikora JL, Fokin A, Golwala NH, Greco AJ, Murthy SN, Nossaman BD, Hyman AL, Kadowitz PJ. Analysis of responses to the Rho-kinase inhibitor Y-27632 in the pulmonary and systemic vascular bed of the rat. Am J Physiol Heart Circ Physiol. 2010; 299:H184–H192. [PubMed: 20435851]
8. Caslin A, Heath D, Smith P. Influence of hypobaric hypoxia in infancy on the subsequent development of vasoconstrictive pulmonary vascular disease in the Wistar albino rat. J Pathol. 1991; 163:133–141. [PubMed: 1901909]
9. Davies SP, Reddy H, Caivano M, Cohen P. Specificity and mechanism of action of some commonly used protein kinase inhibitors. Biochem J. 2000; 351:95–105. [PubMed: 10998351]
10. de Lagausie P, de Buys-Roessingh A, Ferkdadji L, Saada J, Aisenfisz S, Martinez-Vinson C, Fund X, Cayuela JM, Peuchmaur M, Mercier JC, Berrebi D. Endothelin receptor expression in human lungs of newborns with congenital diaphragmatic hernia. J Pathol. 2005; 205:112–118. [PubMed: 15546126]

11. Fagan KA, Oka M, Bauer NR, Gebb SA, Ivy DD, Morris KG, McMurtry IF. Attenuation of acute hypoxic pulmonary vasoconstriction and hypoxic pulmonary hypertension in mice by inhibition of Rho-kinase. Am J Physiol Lung Cell Mol Physiol. 2004; 287:L656–L664. [PubMed: 14977625]
12. Feng J, Ito M, Ichikawa K, Isaka N, Nishikawa M, Hartshorne DJ, Nakano T. Inhibitory phosphorylation site for Rho-associated kinase on smooth muscle myosin phosphatase. J Biol Chem. 1999; 274:37385–37390. [PubMed: 10601309]
13. Gao Y, Portugal AD, Negash S, Zhou W, Longo LD, Usha Raj J. Role of Rho kinases in PKG-mediated relaxation of pulmonary arteries of fetal lambs exposed to chronic high altitude hypoxia. Am J Physiol Lung Cell Mol Physiol. 2007; 292:L678–L684. [PubMed: 17085525]
14. Grimminger F, Weimann G, Frey R, Voswinckel R, Thamm M, Bolkow D, Weissmann N, Muck W, Unger S, Wensing G, Schermuly RT, Ghofrani HA. First acute haemodynamic study of soluble guanylate cyclase stimulator riociguat in pulmonary hypertension. Eur Respir J. 2009; 33:785–792. [PubMed: 19129292]
15. Guilluy C, Sauzeau V, Rolli-Derkinderen M, Guerin P, Sagan C, Pacaud P, Loirand G. Inhibition of RhoA/Rho kinase pathway is involved in the beneficial effect of sildenafil on pulmonary hypertension. Br J Pharmacol. 2005; 146:1010–1018. [PubMed: 16205723]
16. Hamid SA, Bower HS, Baxter GF. Rho kinase activation plays a major role as a mediator of irreversible injury in reperfused myocardium. Am J Physiol Heart Circ Physiol. 2007; 292:H2598–H2606. [PubMed: 17220176]
17. Hampl V, Herget J. Perinatal hypoxia increases hypoxic pulmonary vasoconstriction in adult rats recovering from chronic exposure to hypoxia. Am Rev Respir Dis. 1990; 142:619–624. [PubMed: 2389914]
18. Haworth SG. Pulmonary hypertension in childhood. Eur Respir J. 1993; 6:1037–1043. [PubMed: 8370430]
19. Hemnes AR, Zaiman A, Champion HC. PDE5A inhibition attenuates bleomycin-induced pulmonary fibrosis and pulmonary hypertension through inhibition of ROS generation and RhoA/Rho kinase activation. Am J Physiol Lung Cell Mol Physiol. 2008; 294:L24–L33. [PubMed: 17965319]
20. Ishikura K, Yamada N, Ito M, Ota S, Nakamura M, Isaka N, Nakano T. Beneficial acute effects of Rho-kinase inhibitor in patients with pulmonary arterial hypertension. Circ J. 2006; 70:174–178. [PubMed: 16434811]
21. Ishizaki T, Uehata M, Tamechika I, Keel J, Nonomura K, Maekawa M, Narumiya S. Pharmacological properties of Y-27632, a specific inhibitor of Rho-associated kinases. Mol Pharmacol. 2000; 57:976–983. [PubMed: 10779382]
22. Jankov RP, Kantores C, Belcastro R, Yi M, Tanswell AK. Endothelin-1 inhibits apoptosis of pulmonary arterial smooth muscle in the neonatal rat. Pediatr Res. 2006; 60:245–251. [PubMed: 16857764]
23. Jankov RP, Kantores C, Belcastro R, Yi S, Ridsdale RA, Post M, Tanswell AK. A role for platelet-derived growth factor β-receptor in a newborn rat model of endothelin-mediated pulmonary vascular remodeling. Am J Physiol Lung Cell Mol Physiol. 2005; 288:L1162–L1170. [PubMed: 15722379]
24. Jankov RP, Kantores C, Pan J, Belik J. Contribution of xanthine oxidase-derived superoxide to chronic hypoxic pulmonary hypertension in neonatal rats. Am J Physiol Lung Cell Mol Physiol. 2008; 294:L233–L245. [PubMed: 18083771]
25. Jankov RP, Luo X, Cabacungan J, Belcastro R, Frndova H, Lye SJ, Tanswell AK. Endothelin-1 and O_2-mediated pulmonary hypertension in neonatal rats: a role for products of lipid peroxidation. Pediatr Res. 2000; 48:289–298. [PubMed: 10960492]
26. Jernigan NL, Walker BR, Resta TC. Chronic hypoxia augments protein kinase G-mediated Ca^{2+} desensitization in pulmonary vascular smooth muscle through inhibition of RhoA/Rho kinase signaling. Am J Physiol Lung Cell Mol Physiol. 2004; 287:L1220–L1229. [PubMed: 15310556]
27. Jones JE, Mendes L, Rudd MA, Russo G, Loscalzo J, Zhang YY. Serial noninvasive assessment of progressive pulmonary hypertension in a rat model. Am J Physiol Heart Circ Physiol. 2002; 283:H364–H371. [PubMed: 12063310]

28. Kantores C, McNamara PJ, Teixeira L, Engelberts D, Murthy P, Kavanagh BP, Jankov RP. Therapeutic hypercapnia prevents chronic hypoxia-induced pulmonary hypertension in the newborn rat. Am J Physiol Lung Cell Mol Physiol. 2006; 291:L912–L922. [PubMed: 16829630]
29. Keith IM, Tjen ALS, Kraiczi H, Ekman R. Three-week neonatal hypoxia reduces blood CGRP and causes persistent pulmonary hypertension in rats. Am J Physiol Heart Circ Physiol. 2000; 279:H1571–H1578. [PubMed: 11009443]
30. King AP, Smith P, Heath D. Ultrastructure of rat pulmonary arterioles after neonatal exposure to hypoxia and subsequent relief and treatment with monocrotaline. J Pathol. 1995; 177:71–81. [PubMed: 7472783]
31. Kinoshita E, Kinoshita-Kikuta E, Takiyama K, Koike T. Phosphate-binding tag, a new tool to visualize phosphorylated proteins. Mol Cell Proteomics. 2006; 5:749–757. [PubMed: 16340016]
32. Kobayashi N, Horinaka S, Mita S, Nakano S, Honda T, Yoshida K, Kobayashi T, Matsuoka H. Critical role of Rho-kinase pathway for cardiac performance and remodeling in failing rat hearts. Cardiovasc Res. 2002; 55:757–767. [PubMed: 12176125]
33. Li F, Xia W, Yuan S, Sun R. Acute inhibition of Rho-kinase attenuates pulmonary hypertension in patients with congenital heart disease. Pediatr Cardiol. 2009; 30:363–366. [PubMed: 18953591]
34. Lin G, Craig GP, Zhang L, Yuen VG, Allard M, McNeill JH, MacLeod KM. Acute inhibition of Rho-kinase improves cardiac contractile function in streptozotocin-diabetic rats. Cardiovasc Res. 2007; 75:51–58. [PubMed: 17428455]
35. Manintveld OC, Verdouw PD, Duncker DJ. The RISK of ROCK. Am J Physiol Heart Circ Physiol. 2007; 292:H2563–H2565. [PubMed: 17308009]
36. Matsui T, Amano M, Yamamoto T, Chihara K, Nakafuku M, Ito M, Nakano T, Okawa K, Iwamatsu A, Kaibuchi K. Rho-associated kinase, a novel serine/threonine kinase, as a putative target for small GTP binding protein Rho. EMBO J. 1996; 15:2208–2216. [PubMed: 8641286]
37. McMurtry IF, Abe K, Ota H, Fagan KA, Oka M. Rho kinase-mediated vasoconstriction in pulmonary hypertension. Adv Exp Med Biol. 2010; 661:299–308. [PubMed: 20204738]
38. McNamara PJ, Murthy P, Kantores C, Teixeira L, Engelberts D, van Vliet T, Kavanagh BP, Jankov RP. Acute vasodilator effects of Rho-kinase inhibitors in neonatal rats with pulmonary hypertension unresponsive to nitric oxide. Am J Physiol Lung Cell Mol Physiol. 2008; 294:L205–L213. [PubMed: 18032699]
39. Mohseni-Bod H, Bohn D. Pulmonary hypertension in congenital diaphragmatic hernia. Semin Pediatr Surg. 2007; 16:126–133. [PubMed: 17462565]
40. Mouchaers KT, Schalij I, de Boer MA, Postmus PE, van Hinsbergh VW, Van Nieuw Amerongen GP, Vonk Noordegraaf A, van der Laarse WJ. Fasudil reduces monocrotaline-induced pulmonary arterial hypertension: comparison with bosentan and sildenafil. Eur Respir J. 2010; 36:800–807. [PubMed: 20351034]
41. Murphy JD, Rabinovitch M, Goldstein JD, Reid LM. The structural basis of persistent pulmonary hypertension of the newborn infant. J Pediatr. 1981; 98:962–967. [PubMed: 7229803]
42. Nagaoka T, Fagan KA, Gebb SA, Morris KG, Suzuki T, Shimokawa H, McMurtry IF, Oka M. Inhaled Rho kinase inhibitors are potent and selective vasodilators in rat pulmonary hypertension. Am J Respir Crit Care Med. 2005; 171:494–499. [PubMed: 15563635]
43. Noma K, Oyama N, Liao JK. Physiological role of ROCKs in the cardiovascular system. Am J Physiol Cell Physiol. 2006; 290:C661–C668. [PubMed: 16469861]
44. Oka M, Fagan KA, Jones PL, McMurtry IF. Therapeutic potential of RhoA/Rho kinase inhibitors in pulmonary hypertension. Br J Pharmacol. 2008; 155:444–454. [PubMed: 18536743]
45. Oka M, Homma N, Taraseviciene-Stewart L, Morris KG, Kraskauskas D, Burns N, Voelkel NF, McMurtry IF. Rho kinase-mediated vasoconstriction is important in severe occlusive pulmonary arterial hypertension in rats. Circ Res. 2007; 100:923–929. [PubMed: 17332430]
46. Parker TA, Abman SH. The pulmonary circulation in bronchopulmonary dysplasia. Semin Neonatol. 2003; 8:51–61. [PubMed: 12667830]
47. Rabinovitch M, Gamble WJ, Miettinen OS, Reid L. Age and sex influence on pulmonary hypertension of chronic hypoxia and on recovery. Am J Physiol Heart Circ Physiol. 1981; 240:H62–H72.

48. Rabinovitch M, Keane JF, Norwood WI, Castaneda AR, Reid L. Vascular structure in lung tissue obtained at biopsy correlated with pulmonary hemodynamic findings after repair of congenital heart defects. Circulation. 1984; 69:655–667. [PubMed: 6697454]
49. Rikitake Y, Liao JK. Rho GTPases, statins, and nitric oxide. Circ Res. 2005; 97:1232–1235. [PubMed: 16339495]
50. Robertson TP, Dipp M, Ward JP, Aaronson PI, Evans AM. Inhibition of sustained hypoxic vasoconstriction by Y-27632 in isolated intrapulmonary arteries and perfused lung of the rat. Br J Pharmacol. 2000; 131:5–9. [PubMed: 10960061]
51. Rosenzweig EB, Ivy DD, Widlitz A, Doran A, Claussen LR, Yung D, Abman SH, Morganti A, Nguyen N, Barst RJ. Effects of long-term bosentan in children with pulmonary arterial hypertension. J Am Coll Cardiol. 2005; 46:697–704. [PubMed: 16098438]
52. Sartori C, Allemann Y, Trueb L, Delabays A, Nicod P, Scherrer U. Augmented vasoreactivity in adult life associated with perinatal vascular insult. Lancet. 1999; 353:2205–2207. [PubMed: 10392986]
53. Sasaki Y, Suzuki M, Hidaka H. The novel and specific Rho-kinase inhibitor (S)-(+)-2-methyl-1-[(4-methyl-5-isoquinoline)sulfonyl]-homopiperazine as a probing molecule for Rho-kinase-involved pathway. Pharmacol Ther. 2002; 93:225–232. [PubMed: 12191614]
54. Scherer EQ, Herzog M, Wangemann P. Endothelin-1-induced vasospasms of spiral modiolar artery are mediated by rho-kinase-induced Ca^{2+} sensitization of contractile apparatus and reversed by calcitonin gene-related Peptide. Stroke. 2002; 33:2965–2971. [PubMed: 12468798]
55. Shi J, Wei L. Rho kinase in the regulation of cell death and survival. Arch Immunol Ther Exp (Warsz). 2007; 55:61–75. [PubMed: 17347801]
56. Somlyo AP, Somlyo AV. Ca^{2+} sensitivity of smooth muscle and non-muscle myosin II: modulated by G proteins, kinases, and myosin phosphatase. Physiol Rev. 2003; 83:1325–1358. [PubMed: 14506307]
57. Somlyo AP, Somlyo AV. Signal *transduction* by G-proteins, rho-kinase and protein phosphatase to smooth muscle and non-muscle myosin II. J Physiol. 2000; 522:177–185. [PubMed: 10639096]
58. Stenmark KR, McMurtry IF. Vascular remodeling versus vasoconstriction in chronic hypoxic pulmonary hypertension: a time for reappraisal? Circ Res. 2005; 97:95–98. [PubMed: 16037575]
59. Tamura M, Nakao H, Yoshizaki H, Shiratsuchi M, Shigyo H, Yamada H, Ozawa T, Totsuka J, Hidaka H. Development of specific Rho-kinase inhibitors and their clinical application. Biochim Biophys Acta. 2005; 1754:245–252. [PubMed: 16213195]
60. Thibeault DW, Truog WE, Ekekezie II. Acinar arterial changes with chronic lung disease of prematurity in the surfactant era. Pediatr Pulmonol. 2003; 36:482–489. [PubMed: 14618639]
61. Thomae KR, Nakayama DK, Billiar TR, Simmons RL, Pitt BR, Davies P. The effect of nitric oxide on fetal pulmonary artery smooth muscle growth. J Surg Res. 1995; 59:337–343. [PubMed: 7643591]
62. Tourneux P, Markham N, Seedorf G, Balasubramaniam V, Abman SH. Inhaled nitric oxide improves lung structure and pulmonary hypertension in a model of bleomycin-induced bronchopulmonary dysplasia in neonatal rats. Am J Physiol Lung Cell Mol Physiol. 2009; 297:L1103–L1111. [PubMed: 19837849]
63. van Loon RL, Roofthooft MT, Delhaas T, van Osch-Gevers M, Ten Harkel AD, Strengers JL, Backx A, Hillege HL, Berger RM. Outcome of pediatric patients with pulmonary arterial hypertension in the era of new medical therapies. Am J Cardiol. 2010; 106:117–124. [PubMed: 20609658]
64. Weigand L, Sylvester JT, Shimoda LA. Mechanisms of endothelin-1-induced contraction in pulmonary arteries from chronically hypoxic rats. Am J Physiol Lung Cell Mol Physiol. 2006; 290:L284–L290. [PubMed: 16155085]
65. Weissmann N, Hackemack S, Dahal BK, Pullamsetti SS, Savai R, Mittal M, Fuchs B, Medebach T, Dumitrascu R, Eickels M, Ghofrani HA, Seeger W, Grimminger F, Schermuly RT. The soluble guanylate cyclase activator HMR1766 reverses hypoxia-induced experimental pulmonary hypertension in mice. Am J Physiol Lung Cell Mol Physiol. 2009; 297:L658–L665. [PubMed: 19617308]

66. Yi SL, Kantores C, Belcastro R, Cabacungan J, Tanswell AK, Jankov RP. 8-Isoprostane-induced endothelin-1 production by infant rat pulmonary artery smooth muscle cells is mediated by Rho-kinase. Free Radic Biol Med. 2006; 41:942–949. [PubMed: 16934677]

67. Zeidan A, Javadov S, Karmazyn M. Essential role of Rho/ROCK-dependent processes and actin dynamics in mediating leptin-induced hypertrophy in rat neonatal ventricular myocytes. Cardiovasc Res. 2006; 72:101–111. [PubMed: 16901475]

68. Ziino AJ, Ivanovska J, Belcastro R, Kantores C, Xu EZ, Lau M, McNamara PJ, Tanswell AK, Jankov RP. Effects of Rho-kinase inhibition on pulmonary hypertension, lung growth, and structure in neonatal rats chronically exposed to hypoxia. Pediatr Res. 2010; 67:177–182. [PubMed: 19858775]

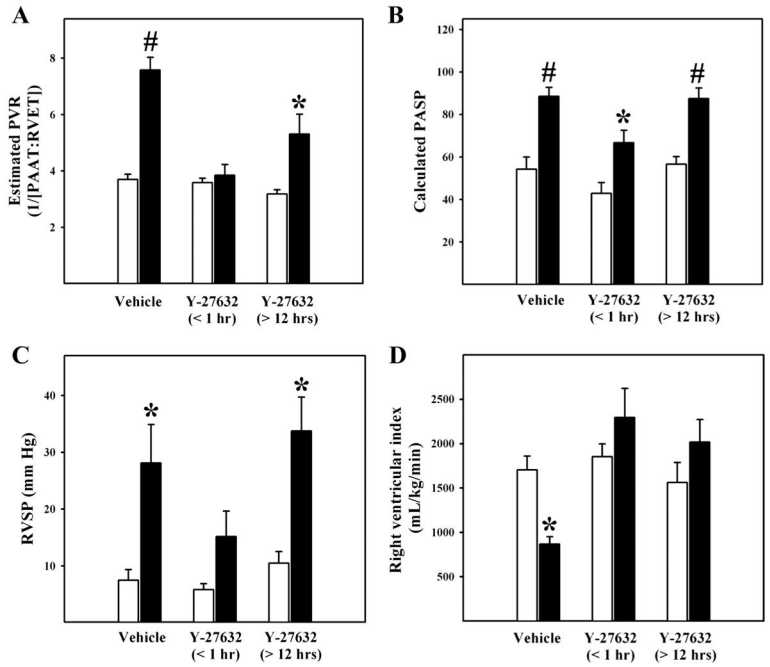

Fig. 1.

Inverse pulmonary arterial acceleration time (PAAT)/right ventricular ejection time (RVET) ratio, as a measure of pulmonary vascular resistance (PVR; *A*); estimated pulmonary arterial systolic pressure (PASP; *B*); right ventricular systolic pressure (RVSP; *C*); and right ventricular performance index (RVI; *D*), as a weight-indexed measure of right ventricular systolic function. Pups were exposed from postnatal *days 1* to *21* to 21% O_2 (air; white bars) or 13% O_2 (hypoxia; black bars) while receiving twice daily subcutaneous injections of 0.9% saline vehicle (vehicle) or 15 mg/kg Y-27632 in 0.9% saline from *days 14* to *21*. Studies were performed within 1 h (<1 h) or 12–18 h (>12 h) from the last dose of Y-27632. Values represent means ± SE for 6–12 animals per group. **P* < 0.05, by ANOVA, compared with respective air-exposed group; #*P* < 0.001, by ANOVA, compared with respective air-exposed group.

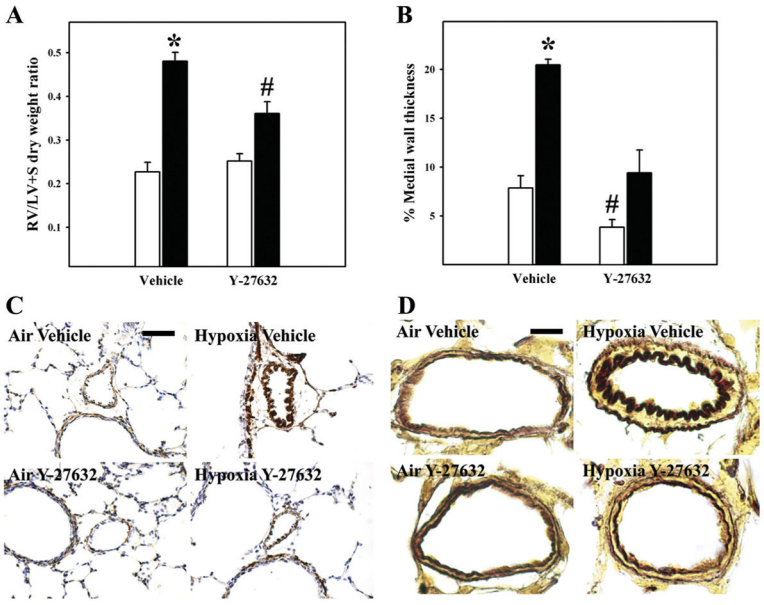

Fig. 2.

Structural changes of chronic pulmonary hypertension. Right ventricle (RV)/left ventricle + septum (LV + S) dry weight ratios as a marker of RV hypertrophy ($n = 7$ to 8 animals/group; *A*) and percent (%) arterial medial wall thickness ($n = 4$ animals/group; *B*) are shown. Values represent means ± SE. Pups were exposed from *postnatal days 1* to *21* to 21% O_2 (air; white bars) or 13% O_2 (hypoxia; black bars) while receiving twice daily subcutaneous injections of 0.9% saline vehicle (vehicle) or 15 mg/kg Y-27632 in 0.9% saline from *days 14* to *21*. *$P < 0.05$, by ANOVA, compared with all other groups; #$P < 0.05$, by ANOVA, compared with air-exposed vehicle-treated group. Representative photomicrographs of α-smooth muscle actin immunohistochemistry (brown stain; bar length = 50 μm; *C*) or Hart's elastin stain (dark brown inner and outer elastic laminae delineating the medial vascular wall; bar length = 10 μm; *D*) demonstrating increased pulmonary arterial wall smooth muscle and medial wall thickening in hypoxia-exposed vehicle-treated animals (hypoxia vehicle), which was largely reversed by treatment with Y-27632 (hypoxia Y-27632), are shown.

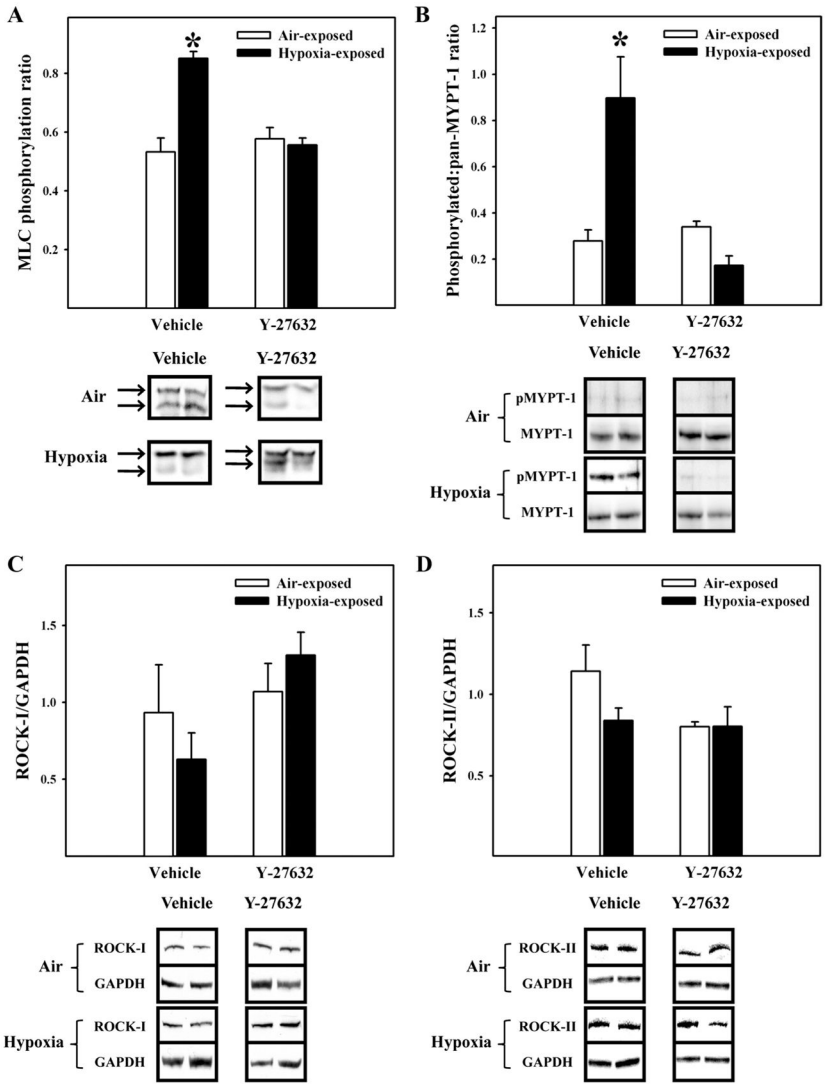

Fig. 3.

Rho-kinase (ROCK) activity and content. Western blot analyses of myosin regulatory light chain (MLC) phosphorylation (*A*) and phosphorylated-to-pan myosin phosphatase target (MYPT)-1 ratio (*B*), as markers of ROCK activity, and ROCK-I (*C*) or ROCK-II (*D*) content in pulmonary arteries are shown. Pups were exposed from *postnatal days 1* to *21* to 21% O_2 (air; white bars) or 13% O_2 (hypoxia; black bars) while receiving twice daily subcutaneous injections of 0.9% saline vehicle (vehicle) or 15 mg/kg Y-27632 in 0.9% saline from *days 14* to *21*. Values represent means ± SE of 4 samples derived from 8 animals per group. $*P <$ 0.05, by ANOVA, compared with all other groups. Representative immunoblots are shown below each graph. For MLC, arrows highlight the upper (phosphorylated) and lower (unphosphorylated) bands, which were resolved by Phos-tag gel electrophoresis.

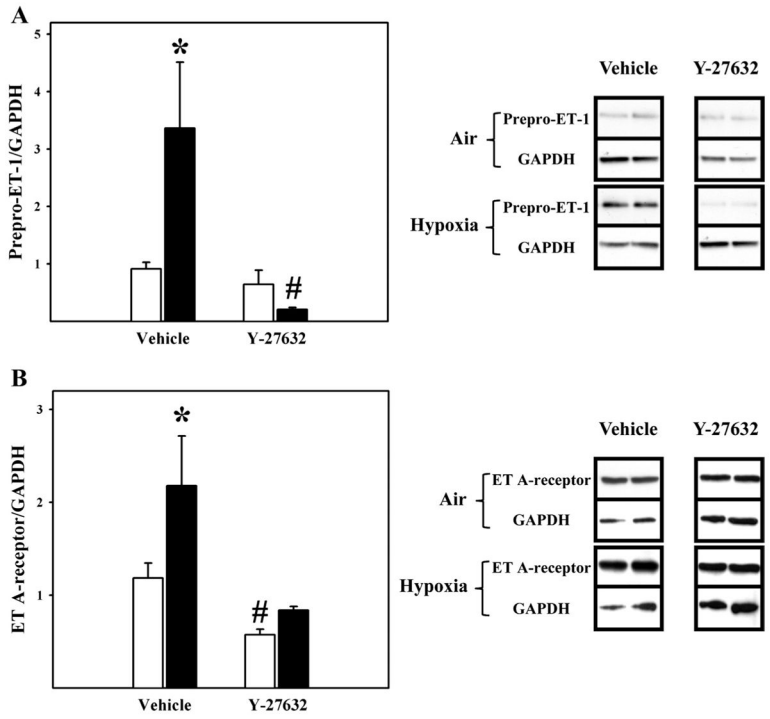

Fig. 4.

Prepro-endothelin (ET)-1 and ET_A receptor content. Western blot analyses of pulmonary arterial prepro-ET-1 (*A*) or ET_A receptor content (*B*) in either air-exposed or 13% O_2-exposed (white bars) animals following twice daily subcutaneous injections of 0.9% saline vehicle (vehicle) or 15 mg/kg Y-27632 in 0.9% saline from *days 14* to *16* are shown. Values represent means ± SE of 4 samples derived from 8 animals per group. $*P < 0.05$, by ANOVA, compared with all other groups; $\#P < 0.05$, by ANOVA, compared with air-exposed vehicle-treated group. Representative immunoblots are shown in the right panels.

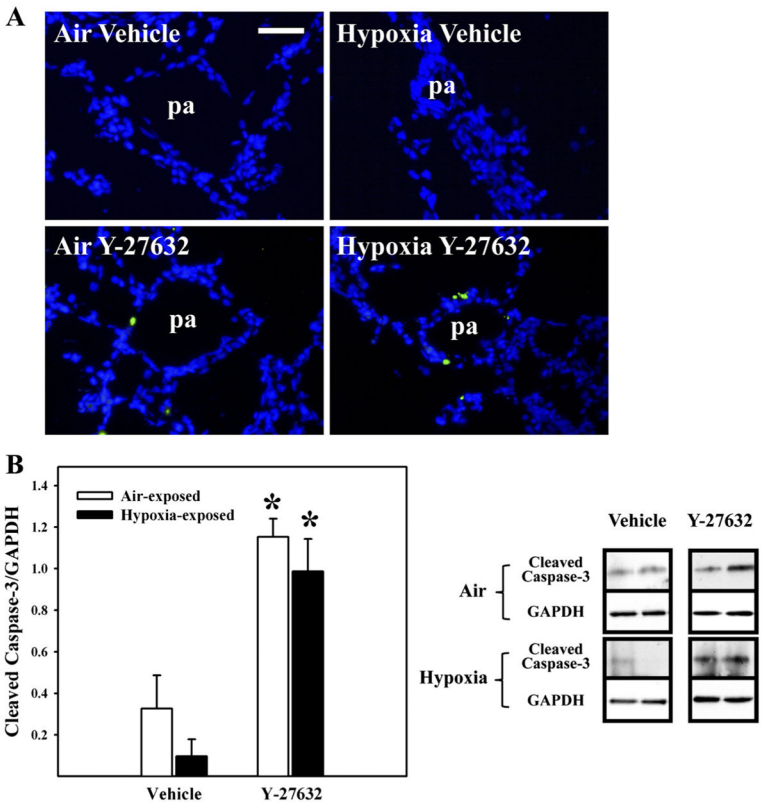

Fig. 5.

Effects of Y-27632 on apoptosis in intrapulmonary arteries (PAs). *A*: representative photomicrographs of fluorescein TUNEL staining on frozen lung sections. Pups were exposed from *postnatal days 1* to *16* to 21% O_2 (air) or 13% O_2 (hypoxia) while receiving twice daily subcutaneous injections of 0.9% saline vehicle (vehicle) or 15 mg/kg Y-27632 in 0.9% saline from *days 14* to *16*. TUNEL-positive (green fluorescent) nuclei were evident in Y-27632-treated animals (greater in hypoxia- than air-exposed animals), which were not observed in vehicle-treated controls. Bar length = 50 μm. *B*: Western blot analyses of cleaved caspase-3, as a marker of apoptosis. Pups were exposed from *postnatal days 1* to *16* to 21% O_2 (air; white bars) or 13% O_2 (hypoxia; black bars) while receiving twice daily subcutaneous injections of 0.9% saline vehicle (vehicle) or 15 mg/kg Y-27632 in 0.9% saline from *days 14* to *16*. Values represent means ± SE of 4 samples derived from 8 animals per group. $*P < 0.01$, by ANOVA, compared with respective vehicle-treated groups. Representative immunoblots are shown in the right panel.

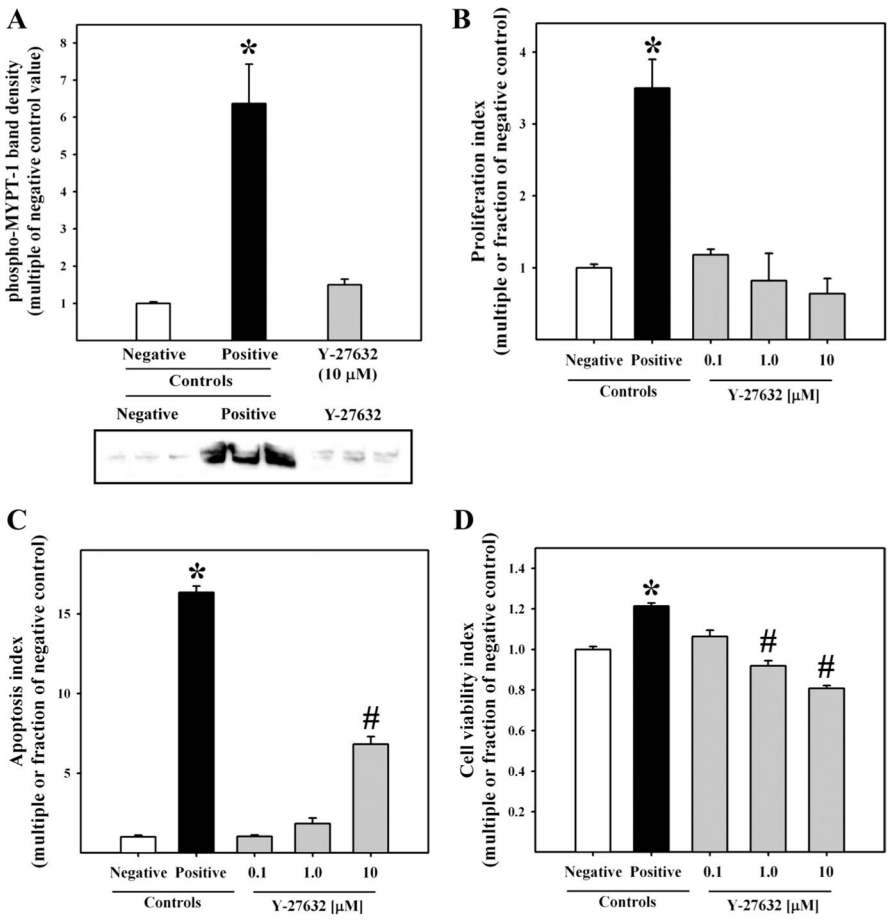

Fig. 6.

Effects of Y-27632 on proliferation, apoptosis, and viability in primary cultured pulmonary artery smooth muscle cells (PASMCs). Analyses of Thr850 phosphorylated MYPT-1, by Western blot, as a marker of ROCK activity ($n = 3$ samples derived from 6 wells/group; immunoblot shown below; *A*), proliferation (*B*), apoptosis (*C*), and viability ($n = 6$ wells/group; *D*) in primary cultured PASMCs are shown. Values represent means ± SE. Cells were treated with DMEM + 0.1% (vol/vol) FBS (negative control; white bars), DMEM + 10% (vol/vol) FBS (positive control for *A*, *B*, and *D*; black bars), DMEM + 10% (vol/vol) FBS + 10 μM paclitaxel (positive control for *C*; black bar), or DMEM + 10% (vol/vol) FBS + Y-27632 (dark gray bars with concentrations indicated). *$P < 0.05$, by ANOVA, compared with all other groups; #$P < 0.05$, by ANOVA, compared with negative control group.

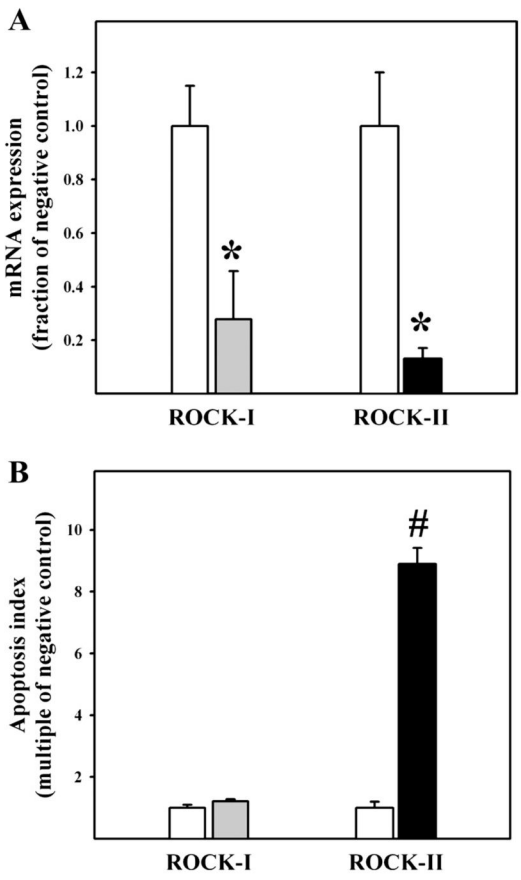

Fig. 7.

Effects of short-interfering RNA (siRNA) knockdown on ROCK isoform expression and apoptosis in primary cultured PASMCs. ROCK-I or -II isoform expression (*A*), quantified by quantitative PCR, and apoptosis in PASMCs cultured from *days 1* to *14* neonatal rats electroporated with control (scrambled) siRNA (white bars; *B*) or siRNAs designed to knockdown ROCK-I (gray bars) or ROCK-II (black bars) are shown. Values represent means ± SE for 4 samples or 6 wells per group. **P* < 0.05, by unpaired *t*-test, compared with control group; #*P* < 0.01, by Mann-Whitney rank sum test, compared with control group.

Table 1

Rat primer sequences for quantitative RT-PCR

Gene	Reference Sequence Accession Number	Forward, 5′-3′	Reverse, 5′-3′
β-Actin	NM_031144	CTGGGTATGGAATCCTGTGG	TAGAGCCACCAATCCACACA
Prepro-endothelin-1	NM_012548	CGTCCCGTATGGACTAGGAA	GTGAGCACACTGGCATCTGT
Endothelin type A receptor	NM_012550	CATGCCTCTGTTGCTGTTGT	TGGTTCTGCTCCTGGTTCTT
Endothelin type B receptor	NM_017333	CCCTGAAGCCATAGGTTTTG	TGCATGAAGGCTGTTTTCTG
Rho-kinase-I	NM_031098	CGACCTGTAACCCAAGGAGA	GGCCTTTGTGATTCTGGAAA
Rho-kinase-II	NM_013022	CGCAGCTCCAGGCCTTGCAT	TCCGCACAGGCAACGACAGC

Table 2

Effects of hypoxia and/or treatment with Y-27632 on mRNA expression of prepro-endothelin-1 and endothelin-1 receptors

Gene	Hypoxia	Air + Y-27632	Hypoxia + Y-27632
Prepro-endothelin-1	2.12 ± 0.35 *	1.05 ± 0.37	0.70 ± 0.27
Endothelin type A receptor	1.15 ± 0.17	0.42 ± 0.18 *	0.36 ± 0.18 *
Endothelin type B receptor	0.87 ± 0.16	1.03 ± 0.17	0.46 ± 0.20

Values are means ± SE of 4 samples per group, relative to control (air-exposed vehicle-treated) group, which was assigned a value of 1.

* $P < 0.05$, by ANOVA, compared with control.